A Wind-Thermal System Design Based on an Energetic and Exergetic Approach

Norouzi, Nima
Department of Energy Engineering and Physics, Amirkabir University of Technology (Tehran Polytechnic), Tehran, I.R. IRAN

Bozorgian, Ali Reza*+
Department of Chemical Engineering, Mahshahr Branch, Islamic Azad University, Mahshahr, I.R. IRAN

ABSTRACT: *Current wind systems are intermittent and cannot be used as the baseload energy source. The research on the concept of wind power using direct thermal energy conversion and thermal energy storage, called Wind-powered Thermal Energy System (WTES), opened the door to a new energy system called Wind-thermal, a strategy for developing baseload wind power systems. The thermal energy is generated from the rotating energy directly at the top of the tower by the heat generator, which is a simple and light electric brake. The rest of the system is the same as the tower-type Concentrated Solar Power (CSP). This paper's results suggest that the energy and exergy performance of the WTES (62.5% and 29.8%) is comparable to that of conventional wind power, which must be supported by the backup thermal plants and grid enhancement. This cogeneration nature of the WTES system makes this system suitable for using wind power as a direct heat source in several heat-demanding processes such as chemical production. Also, the light heat generator reduces some issues of wind power, such as noise and vibration, two main bottlenecks of wind power technology.*

KEYWORDS: *ORC cycle; Wind turbine; Energy analysis; Wind Thermal; Exergy analysis.*

INTRODUCTION

Due to the industrialization of most cities, energy demand grew significantly. The continuous increase in energy demand has led to the widespread use of carbon-containing fossil fuels, which has caused significant damage to the environment and human health. In recent years, many efforts and programs have been made to reduce the use of fossil fuels. Renewable energy sources such as solar and wind have been introduced as reliable sources for clean energy production. Solar power plant technology using parabolic-linear concentrators is the most significant method among thermal-electric methods for renewable energy production[1, 2].

Recently, *Gupta et al.* [1] proposed a system consisting of an organic Rankin cycle with a triple pressure level absorption system and a parabolic-linear solar collector system in 2020. This system generates electricity and refrigeration simultaneously at two different temperatures. This study investigated the effect of different inlet

***** *To whom correspondence should be addressed.*
+ *E-mail: alireza.bozorgian@iau.ac.ir*
1021-9986/2023/5/1666-1677 *12/$/6.02*

parameters such as solar radiation, turbine inlet pressure, turbine outlet pressure, and evaporator temperature on the schematic subsystems. *Kerme et al.* [2] thermodynamically analyzed a multiple power generation system using the thermal energy from a solar system with a parabolic-linear solar collector. The results showed that increasing the turbine inlet temperature increased efficiency and decreased overall energy losses. The results also showed that the two main sources of exergy losses are the solar system and the desalination unit.

Alirahmi et al. [3] proposed a multiple-generation system based on geothermal energy and a parabolic-linear solar collector system for simultaneous electricity generation, cooling load, freshwater, hydrogen, and heat. EES (engineering equation solver) and MATLAB software were interconnected to optimize their research objectives using the Dynamic Exchange Data method. Finally, the system's efficiency and total unit cost were 29.95% and 129.7 $/GJ, respectively. *Alotaibi et al.* [4] investigated the performance of a conventional steam power plant with a regenerative system equipped with a parabolic-linear solar collector system. The system analysis showed that removing the Low-Pressure (LP) turbine increases the performance of the steam power plant up to 9.8 MW/h. The optimal area for the solar system in these conditions was estimated at 25,850 square meters. *Ehyaei et al.* [5] conducted thermodynamic, energy, and exergy, and economic analyses on a linear parabolic solar collector. The optimization results showed that the exergy efficiency, energy efficiency, and costs were 29.29%, 35.55%, and $0.0142/kWh, respectively. *Toghyani et al.* [6] used a nanofluid as a cooling fluid in a parabolic-linear solar collector to cool the solar system and produce hydrogen. The results showed that hydrogen production increases under higher solar intensities because the Rankin cycle transfers more energy to the PEM.

AlZahrani and *Dincer* [7], in 2018, studied the energy and exergy of parabolic-linear solar collectors as part of a solar power plant under different design and performance conditions. Finally, the energy and exergy efficiency rates of 35.66% and 38.55% were reported, respectively. In 2019, *Yilmaz* [8] reviewed the comprehensive thermodynamic performance and economic evaluation of a combined ocean thermal energy system and a wind farm. The results showed that the hybrid system's overall energy and exergy efficiencies are 12.27% and 34.34%, respectively. The cost of the proposed system was reported to be $3.03 per hour. Ishaq and Dincer [9] proposed a new idea for hydrogen production from methanol using wind energy. The proposed system used industrial carbon emissions to produce methanol. EES and Aspen Plus software was used to model and analyze the system. *Bamisile et al.* [10] modeled a power generation system using wind, solar, and biogas energy and analyzed the energy and exergy of the system. The results showed that the system's overall energy efficiency varies from 64.91% to 71.06%, while the exergoeconomic efficiency increases from 31.80% to 53.81%. In 2018, *Kianfard et al.* [11] investigated a renewable system based on thermal energy to produce fresh water and hydrogen. The economic analysis showed that the investment costs per unit of reverse osmosis desalination plant were 56%. The cost of producing freshwater was estimated at 32.73 cents per cubic meter.

Alirahmi and *Assareh* [12] analyzed the energy, exergy, economy, and multiobjective optimization of multiple energy systems, including hydrogen production, freshwater, cooling, heating, hot water, and electricity generation of Dezful City. The two objective functions of this study were exergy and total cost, which were optimized by a genetic algorithm. Finally, the best value for the exergy efficiency was 31.66%, and the total unit rate was 21.9 $/GJ. In 2020, *Mohammadi et al.* [13] designed a combined cycle gas turbine to generate electricity, freshwater, and cooling. The results showed reverse osmosis is more economical than a combined Multi-Effect Distillation And Reverse Osmosis (MED-RO) system. System electricity, water, and cooling costs were also reported at $ 0.0648 per kilowatt-hour, $ 0.7219 per cubic meter, and $ 0.0402 per hour, respectively.

In a study by *Liu et al.* [14], the development of the wind energy industry is seriously restricted by grid connection issues and wind energy generation rejections introduced by the intermittent nature of wind energy sources. To solve these problems, a wind power system integrating with a Thermal Energy Storage (TES) system for District Heating (DH) is designed to use wind power best in the present work. The operation and control of the system are described in detail. A one-dimensional system model is developed based on a generic model library using the object-oriented language Modelica for system modeling. Validations of the main components of the TES module are conducted against experimental results and indicate that the models can be used to simulate the system's operation. The daily performance of the integrated system is analyzed based on a seven-day operation. And the influences of system configurations on the performance of the integrated system are analyzed. The numerical results show that the integrated system can effectively improve the utilization of total wind energy under great wind power rejection.

A paper by *Hemmati* [15] optimizes the cogeneration of a hydro-thermal-wind-solar system. In the proposed hybrid system, the energy storage systems are also incorporated to smooth out the fluctuations of renewable energies. The uncertainties of wind and solar powers are included, and stochastic programming is adopted to deal with the uncertainties. The hydro system comprises two cascade reservoirs. The optimal scheduling of both reservoirs is presented, and the electricity generated by each reservoir is optimized. The optimal scheduling of the thermal unit is also determined. The optimal location, capacity, power, and charging-discharging pattern are determined for battery energy storage systems. The simulations are carried out using an IEEE 69-bus distribution network, and the model is implemented in GAMS software and solved as mixed-integer linear programming. The objective of the problem is to minimize energy costs in the network. The results demonstrate that the proposed stochastic model can successfully optimize the cogeneration of hydro-thermal-wind-solar systems. The planning optimally utilizes energy storage systems to dampen renewable energies' fluctuations and minimize energy costs.

In the studies mentioned above, there is no numerical modeling for wind turbines. It is often assumed that the wind turbine is working under steady operation conditions, and the effect of the changing parameters of the wind turbine on the system was not studied.

In this study, a numerical modeling method is used to model a horizontal-axis wind turbine coupled with a direct heat generator and a Phase Change Material (PCM) storage to enhance the baseload reliability of the wind system, including an Organic Rankine Cycle (ORC), a wind turbine, and a PCM storage. The model studied the effects of the different wind turbine operation conditions on the performance of the described system based on the energy and exergy efficiencies (2E analysis) and finally evaluated the operating conditions for the best overall technical performance of the system.

EXPERIMENTAL SECTION

Case study

Installing renewable energy sources in the electricity grid creates many problems because most renewables are intermittent [14]. This article describes a new idea called wind-powered Thermal Energy (WTES), which was first proposed to solve network problems.

Concentrated Solar Power (CSP) is attracting attention due to its susceptibility to scattering. Some plants can operate with continuous power generation 24 hours a day. Thermal energy storage has already become the second-largest energy storage system in the United States after hydrogen. Solana has been online since 2013 and has a massive 1,680 megawatt-hour power reserve. Total thermal energy storage will almost double in 2015 [3]. Proposals using this practical thermal energy storage are gradually increasing [4-6]. The use of energy storage is also studied from various aspects [7, 8].

This thermal energy storage and a low-cost and lightweight heat generator are key points of WTES. A typical shape of a “specialized thermal type” WTES is shown in Fig. 1. The rotational energy is converted into thermal energy just above the tower. The rest of the system is the same type as the CSP turret [9]. The thermal energy generated is transferred to the base facilities employing a Heat Transfer Fluid (HTF) and produces steam to power the turbine generator when required.

This system is divided into three subsystems and studied in terms of exergy and energy. The subsystems are wind turbine, storage system, and wind turbine system.

Wind turbine energy analysis

If we consider a wind turbine consisting of three general parts of blades, mechanical equipment, and a generator (as shown in Fig. 2), then to analyze the power in each part, energy analysis must be used. The result of using energy analysis is the following Eqs (1) to (4) for turbine power [13].

$$p_w = \frac{1}{2}\rho A \tag{1}$$

$$p_m = p_w \eta_b \tag{2}$$

$$p_G = p_m \eta_m \tag{3}$$

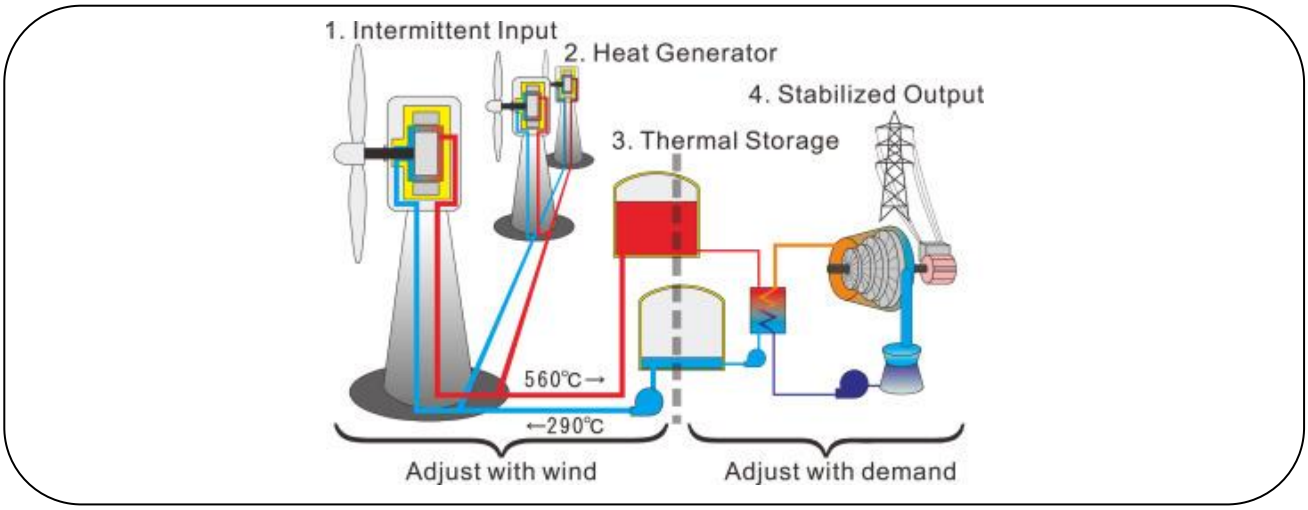

Fig. 1: Schematic of the system.

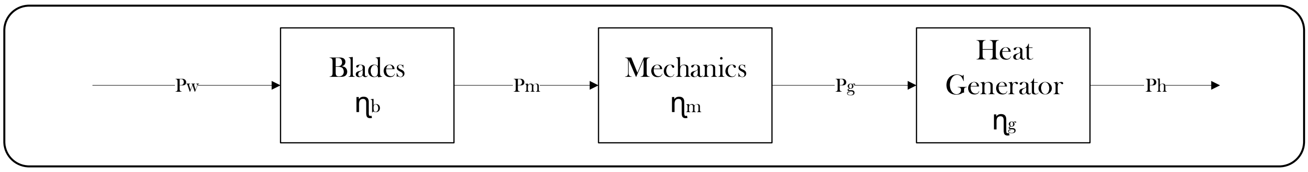

Fig. 2: Schematic of the general parts of a wind turbine.

$$Q_G = p_G\eta_g = \frac{1}{2}\rho AV^3\eta_m\eta_G\eta_b \quad (4)$$

In the above equations, η_b stands for blade efficiency, η_m is the mechanical efficiency of the turbine, η_g is the generator's efficiency, *V* is wind speed, *A* is the effective area of the wind turbine, ρ is the air density, Q_G is turbine output heat, p_G is the power received by the generator, p_m is the power received by mechanical parts, and p_w is the maximum power of the wind[14].

Wind Turbine Exergy Analysis

The exhaust air outlet of the turbine is shown in Eq. (5):

$$EX_{air} = EX_{kinetic} + EX_{potential} + EX_{ph} + EX_{ch} \quad (5)$$

Where *EX* symbolizes the exergy in the above relation, and the substrates of each symbol represent the relevant part (kinetic, potential, physical, and chemical). If we consider the environment as 298 K and air at 1 atm pressure, the chemical and physical exergy of the air will be zero. Because the height of the air does not change, the potential exergy will be zero. So, the air exergy is calculated from $EX_{air} = EX_{kinetic}$ And mass flow and airflow exergy are obtained from the following Eqs (6) and (7) [15]:

$$m = \rho AV_r = \rho\pi R^2 V_r \quad (6)$$

$$EX_{kinetic} = \frac{V_r^2}{2} \quad (7)$$

Where *M*, *R*, and V_r are equal to mass flow, rotor radius, and wind speed at high relationships. In this figure, let's consider the turbine in the simplified form of Fig. 3. The wind turbine consists of blades (assumed to be without friction), mechanical equipment (including shaft, bearing, and gearbox with ηm efficiency) and heat generator with ηG efficiency. As seen from the figure, the energies in the flow are kinetic, work-oriented, and electrical forms that can be fully converted to work, i.e., the current exergy is equal to the content of the flow energy. If for analysis, we consider the system only as a turbine set, then the feed exergy of the system is equal to the state 1 exergy flow, and the product exergy flow is equal to the exergy flow of the state 2. The flows are marked with a number on the figure. The exergy of the flows will be in the form of the following Eqs (7) to (12) [16]:

$$EX_1 = m\left(\frac{V_{in}^2}{2}\right) \quad (7)$$

$$EX_2 = m\left(\frac{V_{out}^2}{2}\right) \quad (8)$$

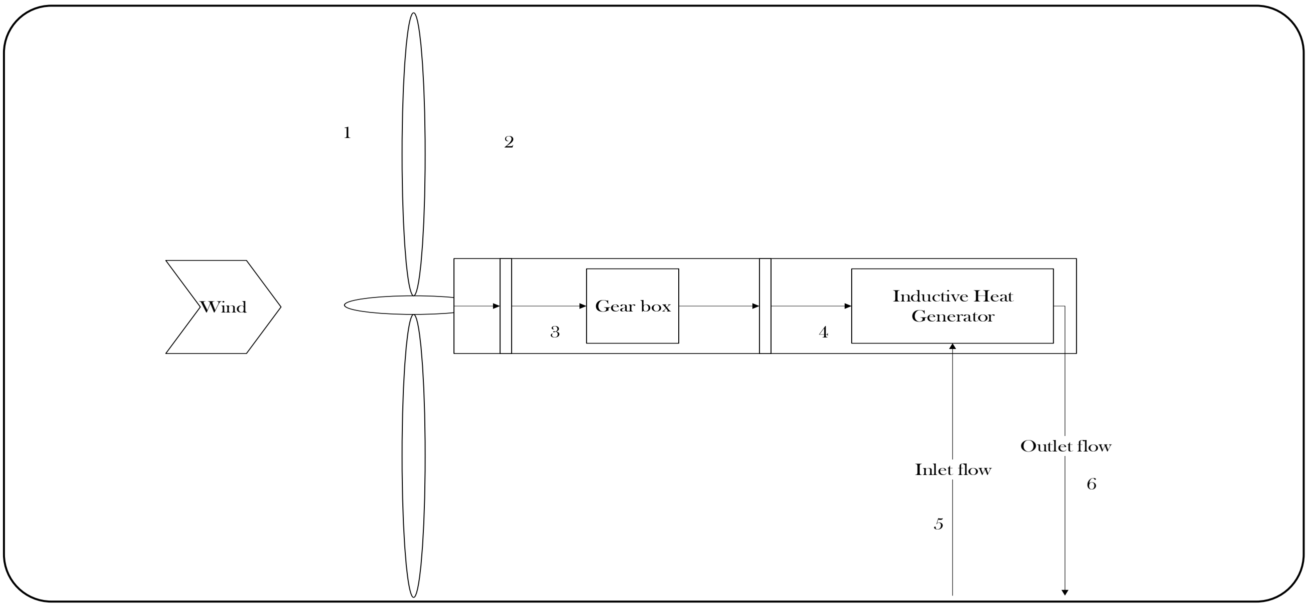

Fig. 3: Schematic of a wind turbine with a display of exergy flows in the turbine assembly.

$$\mathrm{EX_3} = \mathrm{EX_1} - \mathrm{EX_2} \tag{9}$$

$$\mathrm{EX_4} = \eta_m \mathrm{EX_3} \tag{10}$$

$$\mathrm{EX_5} = \text{constant in let water} \sim 0 \tag{11}$$

$$\mathrm{EX_6} = \eta_G \mathrm{EX_5}\left(1 - \frac{T_5}{T_6}\right) \tag{12}$$

In the above equations, *EX* represents the flow of exergy (multiplied by mass flow), and V_{in} and V_{out} are equal to the velocity of the inlet and outlet winds, respectively.

In a wind turbine, the part of the input wind power that is out of the turbine's reach is called the exergy loss and will be equal to the flow exergy of state 1. Also, the part of the exergy, which is lost in the equipment and different parts of the conversion turbine due to friction and inefficiencies of that component and turns into other forms of energy (such as heat), is called exergy destruction, which is equal to the difference in exergy level between the inlet and output flow (as defined by Eq. (13) [17]):

$$\mathrm{EX_D} = \mathrm{EX_{in}} - \mathrm{EX_{out}} \tag{13}$$

In the above relation, EX_{in}, EX_{out}, and EX_D are equal to the output current exergy, the input current exergy, and the exergy destruction, respectively. Therefore, the destruction of the exergies of different parts in a turbine can be calculated from Eqs 14 to 16:

$$\mathrm{EX_D} = \mathrm{EX_3} - \mathrm{EX_4} = \mathrm{EX_3} - \eta_m \mathrm{EX_3} = \mathrm{EX_3}(1 - \eta_m) \tag{14}$$

$$\mathrm{EX_{DG}} = \mathrm{EX_4} - \mathrm{EX_6} = \eta_m \mathrm{EX_3} - \eta_G \mathrm{EX_4} = \eta_m \mathrm{EX_3} - \eta_G \eta_m \left(1 - \frac{T_5}{T_6}\right)\mathrm{EX_3} \tag{15}$$

$$\mathrm{EX_{DG}} = \mathrm{EX_3}\eta_m \left(1 - \eta_G\left(1 - \frac{T_5}{T_6}\right)\right) \tag{16}$$

EX_D, EX_{DG}, and EX_D are the total exergy damage, the generator exergy destruction, and the exergy destruction of the mechanical part, respectively. For each part, a quantity called the destruction ratio is defined, which is equal to the destruction ratio of that part to the system feed exergy. It is defined in Eqs (17) to (20) [18]:

$$y_{D,t} = \frac{E_{D,t}}{E_f} \tag{17}$$

$$y_{D,G} = \frac{E_{D,G}}{E_f} \tag{18}$$

$$y_{D,m} = \frac{E_{D,m}}{E_f} \tag{19}$$

$$y_{D,tot} = \frac{E_{D,tot}}{E_f} \tag{20}$$

Where $y_{D,\,t}$ is equal to the destruction ratio in the *t* part, and *t* can be equal to *G*, *m*, and *tot*, representing the generator, the mechanical part, and the whole system, respectively. Also, the exergy efficiency of the whole turbine system is defined as the ratio between the output current exergy to the feed flow exergy as calculated in Eq. (21):

$$\text{exergy efficiency}_{sys} = \frac{e_p}{e_f} = \frac{EX_6}{EX_1} = \frac{\eta_G \eta_m \left(1 - \frac{T_5}{T_6}\right)}{EX_1} \quad (21)$$

Replacing the new system requires an analysis of many different aspects. Therefore, in the first step of designing the power generation system, the desired system should be adapted to thermodynamics' rules and principles. Due to the CHP system's combination with two different types of generators as the prime movers, energy analysis must be performed. These calculations aim to determine the best combination with the highest output power, recycled heat, overall efficiency, and the lowest fuel consumption of the system.

Storage exergy analysis

Having some practical considerations, a commercial PCM melting point of 250 °C (PlusICE H250) is used as a case study. The supplied exergy by HTF during the charging period, the output exergy at discharging cycle, and the exergetic efficiency of PCM storage can be expressed by the following equations, where T_0, T_6, T_7, and T_m refer to temperatures of ambient, HTF inlet, HTF outlet, and PCM melting point, respectively. Storage heat-loss is considered to be negligible [19]:

Charging is calculated in Eq. (22):

$$EX_{pcm.i} = \dot{m}_{HTF}\, C_{HTF}[(T_6 - T_7) - T_0 \ln(T_6/T_7)] \quad (22)$$

Discharging is calculated in Eq. (23):

$$EX_{pcm.o} = \dot{m}_{HTF}\, C_{HTF}[(T_7 - T_6) - T_0 \ln(T_7/T_6)] \quad (23)$$

Charge and Discharge are calculated in Eq. (24):

$$T_7 = T_m + (T_7 - T_m)e^{-(h_{pcm}A_{pcm}/\dot{m}_{pcm}C_{pcm})} \quad (24)$$

Exergetic PCM storage efficiency is calculated in Eq. (25):

$$\eta_{pcm} = EX_{pcm.o}/EX_{pcm.i} \quad (25)$$

Where $\dot{m_{HTF}} = 6.2\,(kg/s)$. Also, it is assumed that the isothermal PCM melts, and the sensible heat of the PCM is negligible. Moreover, to minimize any unsatisfactory conditions, it is considered that the controlling system would block the storage tank's path as soon as the difference between T_7 and T_m falls below 30°C. The total exergetic outcome of the system with PCM storage is determined as shown in Eq. (26):

$$\text{Total output exergy} = EX_u + EX_{pcm.o} \quad (26)$$

Finally, the overall exergetic efficiency of the whole system is measured by dividing the sum of all output exergy by the amount of input exergy of the solar system.

Results showed that using "PlusICE H250" as the latent heat storage (LHS) for the Shiraz power plant is suitable due to both PCM physical properties and power plant working conditions, such as HTF temperature (see Table 1)[20-31].

Rankin cycle

The heat given to the ORC heat exchanger can be calculated by balancing the energy between the operating fluid and the wind tower fluid at the heat exchanger inlet and outlet obtained from Eq. (27) (see Fig. 4).

$$\dot{Q}_6 = \dot{m}_{turbine}(h_7 - h_5) = \dot{m}_{ORC}(h_8 - h_{11}) \quad (27)$$

where $\dot{m}_{turbine}$ is the mass flow rate of geothermal water, and $\dot{m}_{ORC}$ is the mass flow rate of the ORC cycle. Applying the energy balance, the production capacity of the turbine is obtained from Eq. (28).

$$\dot{W}_t = \dot{W}_{t,isen}\, \eta_t = \eta_t\, \dot{m}_{ORC}\left((h_8 - h_9)\right) \quad (28)$$

The heat given to the cooling water in the condenser is calculated from Eq. (29)[17-22].

$$\dot{Q}_C = \dot{m}_{ORC}\,(h_{10} - h_9) \quad (29)$$

The consumption of pumps in the cycle is calculated from Eq. (30).

$$\dot{W}_P = \dot{W}_{P1} = \frac{\dot{m}_{ORC}}{\eta_P}\,(h_{11} - h_{10}) \quad (30)$$

The net generated power of the ORC cycle is obtained from the algebraic sum of the turbine-generated power and the pump consumption, which is injected into the grid directly as $E_{product}$ calculated in Eq. (31).

$$\dot{W}_{net} = \dot{W}_t - \dot{W}_P = \dot{E}_{Product} \quad (31)$$

The energy efficiency of the Rankin cycle is calculated from Eq. (32)[31-43].

$$\eta_{ORC} = \frac{\dot{W}_{net}}{\dot{Q}_{HX}} \quad (32)$$

Table 1: Selected LHS with PlusICE H250 exergetic analysis results.

Parameter	unit	value
Exergetic efficiency	(%)	85.54
Exergy Loss	(J/s)	30200
$EX_{pcm.o}$	(J/s)	103448
$EX_{pcm.i}$	(J/s)	133567
Density	(kg/m^3)	2380
Latent heat	(kJ/kg)	280
Specific heat	(kJ/kg K)	1.525
Max working temperature	(°C)	600
Melting point	(°C)	250
Material		PlusICE H250

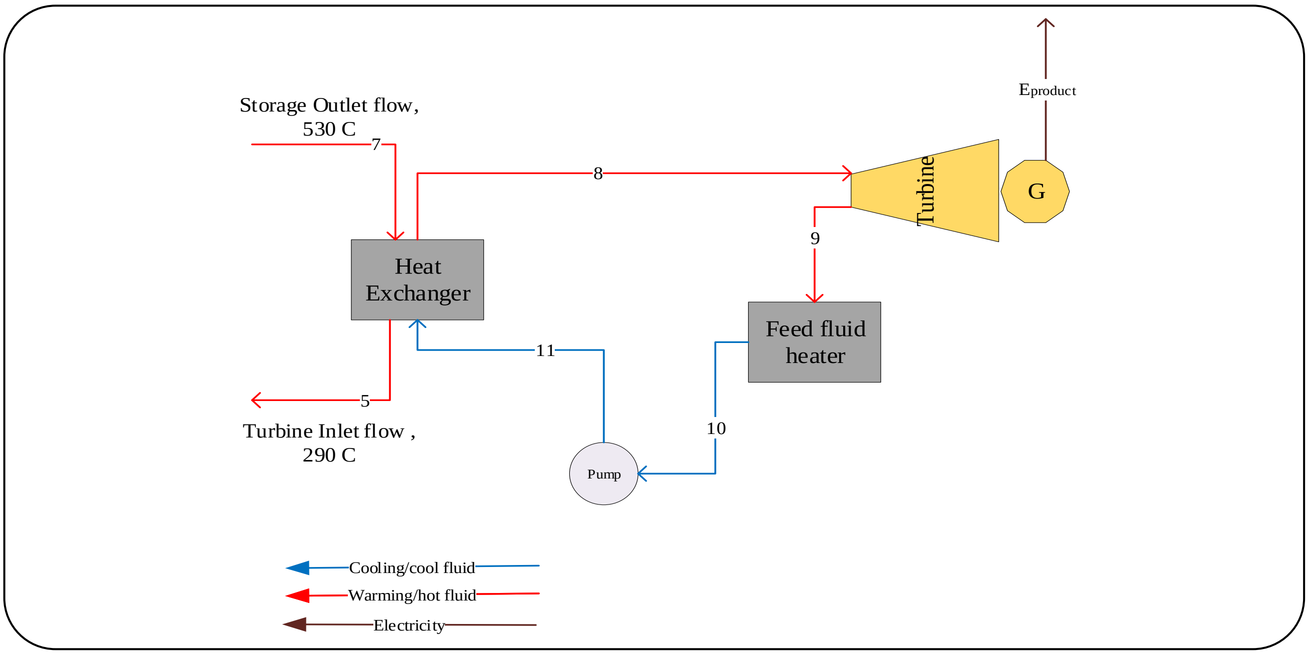

Fig. 4: Schematic of a Rankine system used in the wind turbine system.

RESULTS AND DISCUSSION

Validation

The values and results obtained in this section are first validated before presenting the results. The purpose of accreditation is to ensure the simulation and its results.

Implementing the 2E method can allow us to make satisfactory predictions about the energy produced under different conditions and calculate the wind speed behind the wind turbines to measure the energy and energy efficiency.

Fig. 5 compares the real-state power measurement and the power calculated by the 2E code. As shown in Fig. 5, the 2E code has a good ability to predict the power output. Increasing the wind speed from 4 m/s to 15 m/s results in higher power output at all three tilt angles, whereas reaching a peak at wind speeds of 11.5 m/s has an opposite effect on the power output. On the other hand, increasing the bank angle decreases the power output at all wind speeds. This reduction makes more sense at higher wind speeds. Wind turbines are expected to have the highest performance at a wind speed of 12 m/s and a tilt angle of 5 degrees, producing a power of 140 kW.

Table 2: 2E analysis for wind system in different wind speeds.

Wind speed (m/s)	Energy efficiency (%)	Exergy efficiency (%)	Exergy flow (J/s)	Exergy destruction (J/s)
6	15.1	13.8	55833.8	12037.2
7	34.7	31.5	86571.5	18203.9
8	43.8	41.6	127209.6	24587.9
9	44.8	43.1	179150	33692.4
10	46.8	45.2	243812.1	44596.7
11	45.7	44.4	322612.5	56701.1
12	46.7	44.9	416960.3	71283.5
13	32.8	32.1	528321.2	74462.9
14	25	24.6	658063.4	75354.3
15	18.3	18	807607.5	71847.3

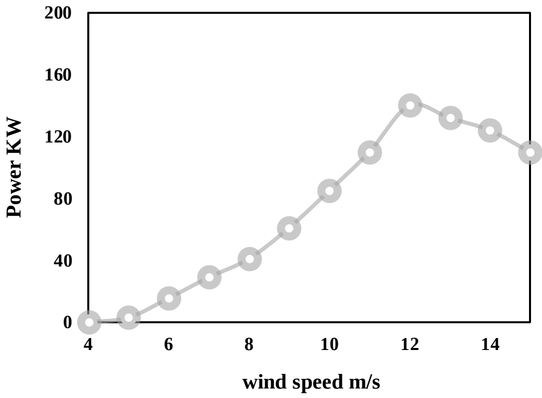

Fig. 5: Comparison of output power between BEM model and experimental data.

Wind Turbine's Energy and Exergy Analyses

As seen in Table 2, the wind speed significantly affects the wind turbine's performance based on energy and exergy efficiencies. It causes a steady rise in exergy flow and destruction. The maximum exergy and energy efficiencies are 44.9 % and 46.7 % at wind speeds of 11.5 m/s, respectively.

Table 3 shows that increasing the pressure change can decrease the wind turbine exergy efficiency while increasing the temperature can increase the efficiency from 42.1% at 5ºC to 43% at 35ºC. However, these changes are not noticeable from the velocity's effect on the wind turbine's exergy efficiency.

Results of the system

By comparing the references and the present work presented in Table 4, it can be seen that there is a good accuracy for the results of the calculated parameters in the present work.

Table 5 shows the performance characteristics of the system. All these values are calculated for four different operating fluids. It is observed that the operating fluid R245fa has the highest energy and exergy efficiency with 49.8% and 27.8%, respectively. Operating fluids R114, R600 and R236fa are also in the next categories regarding performance characteristics. Table 5 shows the lost exergy rate of system components for all operating fluids. Examining the system's exergy based on the above tables shows that the exchanger and the inductive generator have the highest exergy destruction (heat destruction) because both fuels' exergy flow rate and temperature differences are very high. It is also observed that the exergy loss in the exchanger decreases with the change of operating fluid. This trend increases the power by reducing the exergy loss in the exchanger. Comparing the operating fluids exegetically, it is observed that the operating fluid R245fa has the lowest exergy loss and the operating fluid R236fa has the highest exergy loss in the exchanger. Therefore, it can be concluded that the operating fluid with less exergy loss in the exchanger produces more power and higher exergy loss in the wind turbine (see Table 6).

CONCLUSIONS

Thermal backup systems and plants or some energy storage systems are essential when a considerable amount of wind power is injected into the grid. The findings of other studies showed energy costs of the wind with backup thermal, the wind with battery energy storage, and

Table 3: The effect of pressure changes and temperature on the exergy efficiency of wind turbine.

Variables	Exergy efficiency (%)
P= 100 Kpa	44.9
P= 150 Kpa	44.7
P= 200 Kpa	44.6
P= 250 Kpa	44.2
T= 5ºC	44.5
T= 20ºC	44.7
T= 25ºC	44.9
T=35ºC	45.2

Table 4: Performance parameters of organic Rankine cycle with feed fluid recovery and heating.

Parameter	value
Fluid agent	R236fa
Heat Exchanger load (kJ/s)	112
Condenser load (kJ/s)	34.9
Turbine output power (kJ/s)	77.0
Pump power consumption (kJ/s)	2.9
Net power output (kJ/s)	69.9
Energy efficiency (%)	62.4
Mass flow rate of operating fluid (kg/s)	1.1

Table 5: System performance characteristics.

Performance characteristic	R236fa	R600	R114	R245fa
Direct power to grid (kJ/s)	69.9	69.9	69.9	69.9
exchanger heat (kJ/s)	112	112	112	112
Condensing heat (kJ/s)	36.99	36.52	34.93	35.56
Turbine power (kJ/s)	75.01	75.48	77.07	76.44
Pump power (kJ/s)	5.11	5.58	7.17	6.54
Total thermal efficiency (%)	67.0	67.4	68.8	68.3
Rankine cycle exergy efficiency (%)	63.7	64	65.4	64.9
Exergy efficiency with wind system (%)	28.7	28.8	29.4	29.2

Table 6 Loss of exergy rate of different system components, kJ/s.

System components	R236fa	R600	R114	R245fa
Pump	5.21	5.66	7.33	6.54
Storage	12.76	13.21	13.44	13.51
Turbine	5.24	6.64	5.97	6.71
Condenser	116.2	114.1	109.6	109.2
Generator	45.3	46.1	46.4	47.1

Wind powered Thermal Energy System (WTES), which employs inductive heat generators and thermal energy storage systems, are comparable. Also, the results of this study show that the energy and exergy performance of the WTES system is comparable with conventional wind and other energy storage systems. The results of the 2E analysis show that the exergy efficiency of the system is 28.9%, which is a considerably acceptable exergy efficiency. WTES becomes much more attractive when constructed besides CSP and/or bio-mass plants since many elements can be shared. The configuration of WTES has many variations. Employment of the electric and heat generator enables flexible operation. It can even absorb surplus energy from the grid. Employment of the superconducting heat generator realizes high working those variations, including simple thermal specialized types, have much room temperature, i.e., high thermal to electric conversion efficiency.to investigate.

Nomenclature

Turbine	Turbine fluid
C	Condenser
M	Mechanical
cold	Cold stream
HX	Exchanger
in	Inlet
out	Outlet
G	Heat generator
ref	Working fluid
t	Turbine
P p	Pump
q	Specific heat, kJ/kg
Q	Heat rate, kJ/s
s	Specific entropy, kJ/kg.K
P	Pressure, kPa
m	Mass flow rate, kg/s or kg/h
N	Molar flow, mol/s
R	Universal gas constant, kJ/kg.K
Tm	Melting point temperature, °C
To	Environment temperature, °C
Ti	Inner temperature, °C
T_0	Ambient temperature, K
η	Efficiency, %
$E_{product}$	Power to the grid, kJ/s
mean	Average
h	Specific enthalpy, kJ/kg.K
EX	Exergy flow, kJ/s or J/s
EXpcm.i	Eexergy supplied to the PCM during charging, kJ/s
EXpcm.o	Exergy output from the PCM during discharging, kJ/s

Received : May 25, 2022 ; Accepted : Sep. 26, 2022

REFERENCES

[1] Gupta D.K., Kumar R., Kumar N., Performance Analysis of PTC Field Based Ejector Organic Rankine Cycle Integrated with a Triple Pressure Level Vapor Absorption System (EORTPAS). *Engineering Science and Technology, an International Journal*, **23(1)**: 82-91 (2020).

[2] Kerme E.D., Orfi J., Fung A.S., Salilih E.M., Khan S.U.-D., Alshehri H., Ali E., Alrasheed M., Energetic and Exergetic Performance Analysis of a Solar Driven Power, Desalination and Cooling Poly-Generation System, *Energy*, **196**: 117150 (2020).

[3] Alirahmi S.M., Rahmani Dabbagh S., Ahmadi P., Wongwises S., Multiobjective Design Optimization of a Multi-Generation Energy System Based on Geothermal and Solar Energy, *Energy Convers. Manag.*, **205**: 112426 (2020).

[4] Alotaibi S., Alotaibi F., Ibrahim O.M., Solar-Assisted Steam Power Plant Retrofitted with Regenerative System Using Parabolic Trough Solar Collectors, *Energy Reports*, **6**: 124-133 (2020).

[5] Ehyaei M.A., Ahmadi A., El Haj Assad M., Salameh T., Optimization of Parabolic Through Collector (PTC) with Multi Objective Swarm Optimization (MOPSO) and Energy, Exergy and Economic Analyses, *Journal of Cleaner Production*, **234**: 285-296 (2019).

[6] Toghyani S., Afshari E., Baniasadi E., Shadloo M.S., Energy and Exergy Analyses of a Nanofluid Based Solar Cooling and Hydrogen Production Combined System, *Renewable Energy*, **141**: 1013-1025 (2019).

[7] Al Zahrani A.A., Dincer I., Energy and Exergy Analyses of a Parabolic Trough Solar Power Plant Using Carbon Dioxide Power Cycle, *Energy Convers. Manag.*, **158**: 476-488 (2018).

[8] Yilmaz F., Energy, exergy and Economic Analyses of a Novel Hybrid Ocean Thermal Energy Conversion System for Clean Power Production. *Energy Conversion and Management*, **196**: 557-566 (2019).

[9] Ishaq, H., Dincer, I., Evaluation of a Wind Energy Based System for Cogeneration of Hydrogen and Methanol Production, *International Journal of Hydrogen Energy*, **45(32)**: 15869-15877 (2020).

[10] Bamisile O., Huang Q., Li J., Dagbasi M., Desire Kemena A., Abid M., Hu W., Modelling and Performance Analysis of an Innovative CPVT, Wind and Biogas Integrated Comprehensive Energy System: An Energy and Exergy Approach, *Energy Conversion and Management*, **209**: 112611 (2020).

[11] Kianfard H., Khalilarya S., Jafarmadar S., Exergy and Exergoeconomic Evaluation of Hydrogen and Distilled Water Production *via* Combination of PEM Electrolyzer, RO Desalination Unit and Geothermal Driven Dual Fluid ORC, *Energy Conversion and Management*, **177**: 339-349 (2018).

[12] Alirahmi S.M., Assareh E., Energy, Exergy, and Exergoeconomics (3E) Analysis and Multiobjective Optimization of a Multi-Generation Energy System for Day and Night Time Power Generation - Case Study: Dezful City, *International Journal of Hydrogen Energy*, **45(56)**: 31555-31573 (2020).

[13] Mohammadi K., Khaledi M.S.E., Saghafifar M., Powell K., Hybrid Systems Based on Gas Turbine Combined Cycle for Trigeneration of Power, Cooling, and Freshwater: A Comparative Techno-Economic Assessment. *Sustainable Energy Technologies and Assessments*, **37**: 100632 (2020).

[14] Liu C., Cheng M.S., Zhao B.C., Dai Z.M., A Wind Power Plant with Thermal Energy Storage for Improving the Utilization of Wind Energy, *Energies*, **10(12)**: 2126 (2017).

[15] Hemmati R., Optimal Cogeneration and Scheduling of Hybrid Hydro-Thermal-Wind-Solar System Incorporating Energy Storage Systems, *Journal of Renewable and Sustainable Energy*, **10(1)**: 014102 (2018).

[16] Hoseinzadeh S., Stephan Heyns P., Advanced Energy, Exergy, and Environmental (3E) Analyses and Optimization of a Coal-Fired 400 MW Thermal Power Plant, *Journal of Energy Resources Technology*, **143(8)**: 082106 (2021).

[17] Hoseinzadeh S., Yargholi R., Kariman H., Heyns P.S., Exergoeconomic Analysis and Optimization of Reverse Osmosis Desalination Integrated with Geothermal Energy, *Environmental Progress & Sustainable Energy*, **39(5)**: e13405 (2020).

[18] Hoseinzadeh S., Stephan Heyns P., Development of a Model Efficiency Improvement for the Designing of Feedwater Heaters Network in Thermal Power Plants, *Journal of Energy Resources Technology*, **144(7)**: 072102 (2022).

[19] Kariman H., Hoseinzadeh S., Heyns P.S., Energetic and Exergetic Analysis of Evaporation Desalination System Integrated with Mechanical Vapor Recompression Circulation, *Case Studies in Thermal Engineering*, **16**: 100548 (2019).

[20] Kariman H., Hoseinzadeh S., Shirkhani A., Heyns P S., Wannenburg J., Energy and Economic Analysis of Evaporative Vacuum Easy Desalination System with Brine Tank, *Journal of Thermal Analysis and Calorimetry*, **140(4)**: 1935-1944 (2019).

[21] Mahmoudan A., Esmaeilion F., Hoseinzadeh S., Soltani M., Ahmadi P., Rosen M., A Geothermal and Solar-Based Multigeneration System Integrated with a TEG unit: Development, 3E Analyses, and Multiobjective Optimization, *Applied Energy*, **308**: 118399 (2022).

[22] Mahmoudan A., Samadof P., Hosseinzadeh S., Garcia D.A., A Multigeneration Cascade System Using Ground-Source Energy with Cold Recovery: 3E Analyses and Multiobjective Optimization, *Energy*, **233**: 121185 (2021).

[23] Kariman H., Hoseinzadeh S., Heyns P.S., Sohani A., Modeling and Exergy Analysis of Domestic MED Desalination with Brine Tank, *Desalination and Water Treatment*, **197**: 1-13 (2020).

[24] Okazaki T., Shirai Y., Nakamura T., Concept Study of Wind Power Utilizing Direct Thermal Energy Conversion and Thermal Energy Storage, *Renewable Energy*, **83**: 332-338 (2015).

[25] Razmi A.R., Janbaz M., Exergoeconomic Assessment with Reliability Consideration of a Green Cogeneration System Based on Compressed Air Energy Storage (CAES), *Energy Conversion and Management*, **204**: 112320 (2020).

[26] Rashidi H., Khorshidi J., Exergoeconomic Analysis and Optimization of a Solar Based Multigeneration System Using Multiobjective Differential Evolution Algorithm, *Journal of Cleaner Production*, **170**: 978-990 (2018).

[27] Nemati A., Sadeghi M., Yari M., Exergoeconomic Analysis and Multiobjective Optimization of a Marine Engine Waste Heat Driven RO Desalination System Integrated with an Organic Rankine Cycle Using Zeotropic Working Fluid, *Desalination*, **422**: 113-123 (2017).

[28] Naseri, A., Bidi, M., Ahmadi, M. H., and Saidur, R., Exergy Analysis of a Hydrogen and Water Production Process by a Solar-Driven Transcritical CO_2 Power Cycle with Stirling Engine, *Journal of Cleaner Production*, **158**: 165-181 (2017).

[29] Norouzi, N., The Pahlev Reliability Index: A Measurement for the Resilience of Power Generation Technologies Versus Climate Change, *Nuclear Engineering and Technology*, **53(5)**: 1658-1663 (2021).

[30] Khajehpour H., Norouzi N., Bashash Jafarabadi Z., Valizadeh G., Hemmati M.H., Energy, Exergy, and Exergoeconomic (3E) Analysis of Gas Liquefaction and Gas Associated Liquids Recovery Co-Process Based on the Mixed Fluid Cascade Refrigeration Systems, *Iran. J. Chem. Chem. Eng. (IJCCE)*, **41(4):** 1391-1410 (2021).

[31] Habibollahzade A., Gholamian E., Ahmadi P., Behzadi A., Multi-Criteria Optimization of an Integrated Energy System with Thermoelectric Generator, Parabolic Trough Solar Collector and Electrolysis for Hydrogen Production, *International Journal of Hydrogen Energy*, **43(31)**: 14140-14157 (2018).

[32] Raei B., Ghadi A., Bozorgian A., "Heat Integration of Heat Exchangers Network Using Pinch Technology", in: *19th International Congress of Chemical and Process Engineering CHISA*, (2010).

[33] Pourabadeh A., Nasrollahzadeh B., Razavi R., Bozorgian A., Najafi M., A.Oxidation of FO and N_2 Molecules on the Surfaces of Metal-Adopted Boron Nitride Nanostructures as Efficient Catalysts, *J. Struct. Chem.*, **59**: 1484–1491 (2018).

[34] Esmaeili Bidhendi M., Asadi Z., Bozorgian A., et al., New Magnetic Co_3O_4/Fe_3O_4 Doped Polyaniline Nanocomposite for the Effective and Rapid Removal of Nitrate Ions from Ground Water Samples, *Environ. Prog. Sustainable Energy*, **39**: e13306 (2019).

[35] Bozorgian A., Arab Aboosadi Z., Mohammadi A., Honarvar B., Azimi A., Optimization of Determination of CO2 Gas Hydrates Surface Tension in the Presence Of Non-Ionic Surfactants and TBAC, *Eurasian Chem. Commun.*, **2**: 420-426 (2020).

[36] Mashhadizadeh J., Bozorgian A., Azimi A., Investigation of the Kinetics of Formation of Clatrit-Like Dual Hydrates TBAC in the Presence of CTAB, *Eurasian Chem. Commun.*, **2**: 536-547 (2020).

[37] Norouzi N., Bozorgian A., Dehghani M., Best Option of Investment in Renewable Energy: A Multicriteria Decision-Making Analysis for Iranian Energy Industry, *Journal of Environmental Assessment Policy and Management*, **22(1-2)**: 2250001 (2020).

[38] Norouzi N., Ebadi A., Bozorgian A., Hoseyni S.J., Vessally E., Energy and Exergy Analysis of Internal Combustion Engine Performance of Spark Ignition for Gasoline, Methane, and Hydrogen Fuels, *Iran. J. Chem. Chem. Eng. (IJCCE)*, **40**: 1909-1930 (2021).

[39] Bozorgian A., Arab Aboosadi Z., Mohammadi A., Honarvar B., Azimi A., Statistical Analysis of the Effects of Aluminum Oxide (Al_2O_3) Nanoparticle, TBAC, and APG on Storage Capacity of CO_2 Hydrate Formation, *Iran. J. Chem. Chem. Eng. (IJCCE)*, **41**: 220-231 (2022).

[40] Ahmadpour A., Bozorgian A., Eslamimanesh A., Mohammadi A.H., Photocatalytic Treatment of Spontaneous Effluent of Petrochemical Effluents by TiO2 CTAB Synthetic Nanoparticles, *Desalin. Water Treat.*, 249: 297-308 (2022).

[41] Norouzi N., Ebadi A., Bozorgian A., Hoseyni S.J., Vessally E., Cogeneration System of Power, Cooling, and Hydrogen from Geothermal Energy: An Exergy Approach, *Iran. J. Chem. Chem. Eng. (IJCCE)*, **41**: 706-721 (2022).

[42] Bozorgian A., Arab Aboosadi Z., Mohammadi A., Honarvar B., Azimi A., Determination of CO2 gas Hydrates Surface Tension in the Presence of Nonionic Surfactants and TBAC, *Rev. Roum. Chim.*, **65**: 1061-1065 (2020).

[43] Kanani M., Kanani N., Batooie N., Bozorgian A., Barghi A., Rezania Sh., Removal of Rhodamine 6G Dye Using One-Pot Synthesis of Magnetic Manganese Graphene Oxide: Optimization by Response Surface Methodology, *Environ. Nanotechnol., Monit. Manage.*, **18**: 100709 (2022).